The Binding Dynamics of Tropomyosin on Actin

Andrej Vilfan

Cavendish Laboratory, Madingley Road, Cambridge CB3 0HE, United Kingdom

ABSTRACT   We discuss a theoretical model for the cooperative binding dynamics of tropomyosin to actin filaments. Tropomyosin binds to actin by occupying seven consecutive monomers. The model includes a strong attraction between attached tropomyosin molecules. We start with an empty lattice and show that the binding goes through several stages. The first stage represents fast initial binding and leaves many small vacancies between blocks of bound molecules. In the second stage the vacancies annihilate slowly as tropomyosin molecules detach and reattach. Finally, the system approaches equilibrium. Using a grain-growth model and a diffusion-coagulation model we give analytical approximations for the vacancy density in all regimes.

INTRODUCTION

Tropomyosin (TM) is the protein that plays the key role in the regulation of muscle contraction (Lehrer and Geeves, 1998). It comes in a rod-like form and binds to the groove of each side of double-helical actin filaments (Fig. 1). Actin filaments give the cytoskeleton its mechanical stability and serve as tracks for motor proteins from the myosin family, especially in muscle cells. In muscle, each tropomyosin molecule covers seven actin monomers (McLachlan and Stewart, 1976; Hitchcock-deGregori and Varnell, 1990). Other tropomyosins covering six and five monomers exist as well (for review, see Hitchcock-deGregori (1994)), but for specificity we will focus on TM covering seven actin subunits. Together with the associated protein troponin, TM on actin can switch between two laterally shifted conformations (Vibert et al., 1997; Lehman et al., 2000). The equilibrium between these two conformations is strongly influenced by the concentration of Ca^{2+} ions. As one conformation obstructs the strong binding of myosin to actin (Geeves and Lehrer, 1994; Lehrer and Geeves, 1998), this provides the mechanism of calcium-mediated activation of myosin in skeletal muscle cells. The regulation of myosin activity has been widely studied using actin-tropomyosin filaments assembled in vitro (Fraser and Marston, 1995; Gordon et al., 1997). Other functions of TM might include the stabilization of actin against fragmentation and actin assembly (Lazarides, 1976; Weigt et al., 1991).

The binding of tropomyosin to actin has been studied in equilibrium (Wegner, 1979; Hill et al., 1992) as well as dynamically (Wegner and Ruhnau, 1988; Weigt et al., 1991) and has been found to be highly cooperative (Wegner, 1979; Hill et al., 1992). But the way that TM binds to actin is not simple. As each TM molecule occupies seven actin monomers, an obvious problem is that sometimes a gap of one to six monomers, too short for another TM molecule to be inserted, can remain on actin. It has been suggested (Weigt et al., 1991) that these gaps could play an important role by regulating the binding of α-actinin and the fragmentation kinetics of actin.

In this article, we study a theoretical model for the dynamics of binding of TM to actin based on the reaction kinetics shown in Fig. 2, first proposed by Wegner and coworkers (Wegner, 1979; Weigt et al., 1991). The equilibrium distribution of bound molecules and vacancies has been known exactly for a long time (Wegner, 1979) and represents a special case of a more general model solved by McGhee and von Hippel (1974). However, as we have previously shown in the context of kinesin on microtubules (Vilfan et al., 2001b), the time necessary to reach the equilibrium state can be very long. There are many similarities between the binding of dimeric kinesin on microtubules and TM on actin. In both situations there is an initial period in which all gaps that are wide enough to accept a new molecule get filled. The dynamics within this period has been directly experimentally observed using fluorescent techniques (Weigt et al., 1991). After the initial period, only vacancies stretching over one to six actin monomers, too small for another TM molecule to fit in, remain. They get healed out in a much slower annealing process in which bound molecules detach and others reattach at other places. This process takes place on a much slower time scale. The annealing process is finished when the system reaches the equilibrium state. Despite the similarities with the binding
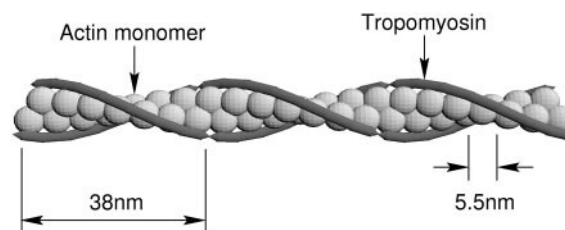
FIGURE 1   TM binds on actin polymers on each side of the double helix. One TM molecule thereby occupies seven actin monomers.
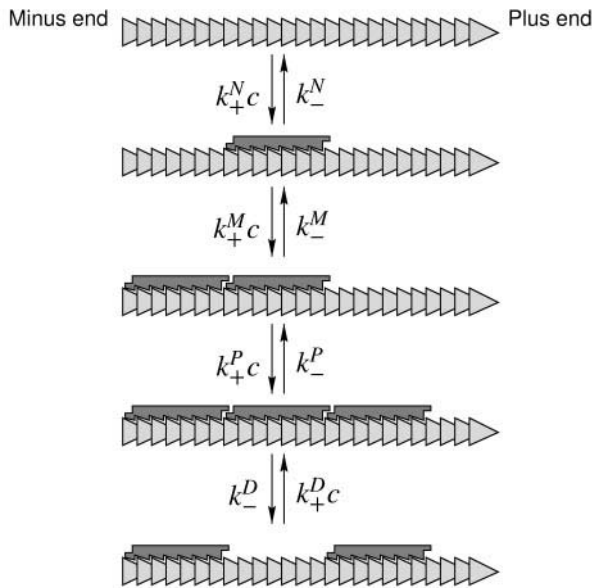
FIGURE 2   Reaction scheme for all binding and unbinding processes of TM on actin. The binding (unbinding) rate for an isolated site is $k_+^N c$ (k_-^N), at the "−" side of another bound TM molecule $k_+^M c$ (k_-^M), at the "+" side $k_+^P c$ (k_-^P), and between two bound TM molecules $k_+^D c$ (k_-^D). c denotes the concentration of TM in solution.

of kinesin onto microtubules, there are also important differences: 1) the TM molecules occupy seven instead of two binding sites; 2) kinesin dimers can bind with one head as well as with two, whereas TM must either bind all sites or be fully detached; and 3) the interaction between bound tropomyosin molecules is much stronger. In our theoretical analysis we make reasonable simplifications justified by experimental observations and then use results from diffusion-annihilation models to find an analytical solution for the dynamics in our model. The central result is the prediction of the number of defects (gaps between contiguous blocks of TM) as a function of time for a given solution concentration.

The fact that a TM molecule occupies seven binding sites makes it especially interesting from the theoretical point of view. The size seven lies between the simple monomeric or dimeric and continuous models. We have shown previously that the relaxational behavior of the dimer adsorption-desorption model can be explained by a mapping onto the $A + A \rightarrow 0$ diffusion-annihilation model (Vilfan et al., 2001a). The gap density decays with a power-law $\propto t^{-1/2}$ before it approaches the final equilibrium value. This behavior remains qualitatively valid even if there is an attractive interaction between adsorbed dimers. If one introduces a strong diffusion of adsorbed dimers the power-law decay is preceded by a mean-field regime in which $n_G \propto t^{-1}$ (Privman and Nielaba, 1992). On the other hand, noninteracting k-mers ($k > 3$) are always well described with the mean-field kinetics of the model $kA \rightarrow 0$, which predicts a gap density

decay $\propto t^{-1/(k-1)}$ (Nielaba and Privman, 1992). In the continuous limit, also called continuous sequential adsorption (CSA) or "car parking problem," the length of unoccupied space decays as $\propto 1/\log t$ in the mean-field regime (Krapivsky and Ben-Naim, 1994; Jin et al., 1994). We will show that our model ($k = 7$ with strong attractive interaction) differs from all models mentioned above and that it maps onto a $A + A \rightarrow \frac{5}{6} A$ model, which includes particle annihilation as well as coagulation.

DEFINITION OF THE MODEL

Our model is based on the reaction scheme shown in Fig. 2 and is defined as follows. We assume that there is no interaction between bound TM molecules on the opposite sides of the actin polymer and therefore describe actin as two independent one-dimensional binding lattices. We further assume that TM molecules can bind to actin only with their whole length, thereby occupying seven binding actin monomers. The rate at which a TM molecule binds to a group of seven free binding sites on actin is $k_+^N c$ where c denotes the TM concentration. The rate for the reverse reaction, i.e., the detachment of a TM molecule without neighbors, is k_-^N. The rate at which new TM molecules bind beside already bound ones (we call such sites single-contiguous binding sites) will be denoted as $k_+^P c$ (the rate at which the new TM binds on the plus side of a previously occupied block) and $k_+^M c$ (on the minus side). The reverse reaction rates are k_-^P and k_-^M. It is reasonable to assume that the binding constants are only influenced by nearest neighbors. Finally the attachment rate in a gap of exactly seven lattice sites will be $k_+^D c$ and the detachment rate in the middle of a contiguous block k_-^D. The principle of detailed balance states that the ratio between the binding and unbinding rate depends only on the free energy difference and therefore has the same value regardless whether a molecule binds on the plus or minus side of an occupied block

$$\frac{k_+^M}{k_-^M} = \frac{k_+^P}{k_-^P} = K = \frac{k_+^N}{k_-^N} \exp \frac{J}{k_B T} = K^N \exp \frac{J}{k_B T} = K^N \gamma. \quad (1)$$

Here J denotes the coupling energy between two TM molecules on actin and $\gamma = \exp(J/k_B T)$ the cooperativity coefficient (Hill, 1985). The coupling energy from both ends is additive, therefore

$$\frac{k_+^D}{k_-^D} = K^D = \frac{k_+^N}{k_-^N} \exp \frac{2J}{k_B T} = K^N \gamma^2. \quad (2)$$

In the following we will assume a strong interaction between bound molecules, $\gamma \gg 1$. The assumption is well justified because the cooperativity coefficient has been determined to be between $\gamma = 600$ and $\gamma = 1000$ by Wegner (1979) and approximately $\gamma = 100$ by Hill et al. (1992). The
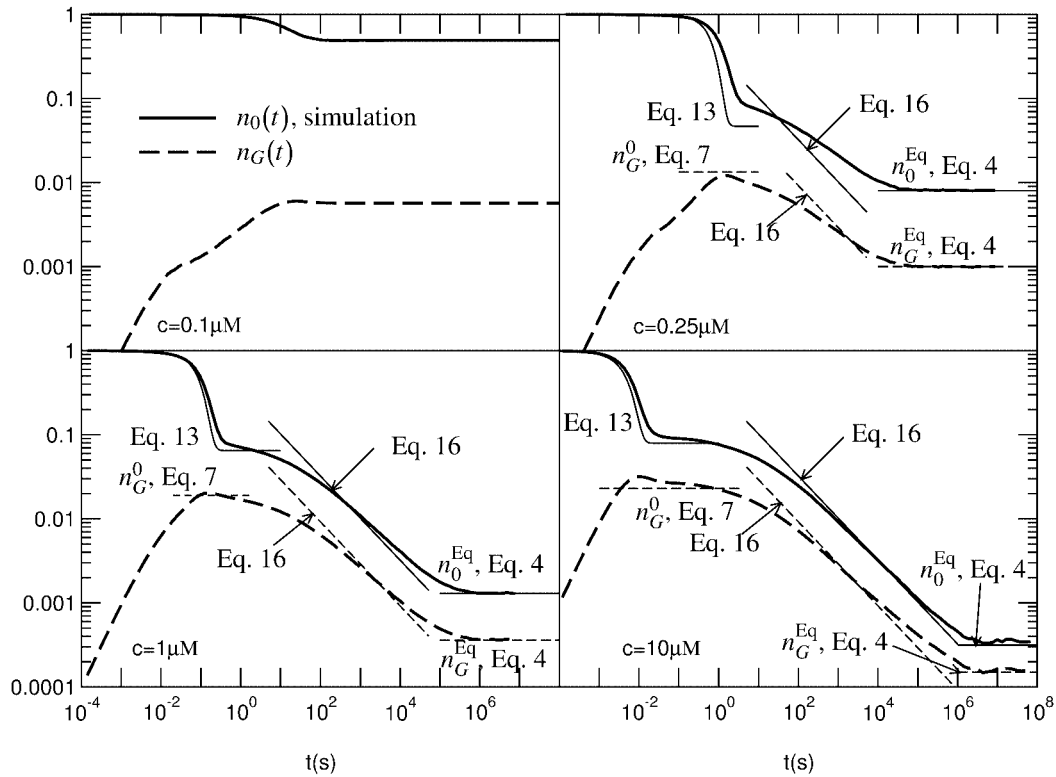
FIGURE 3 Gap density ($n_G(t)$, *dashed line*) and fraction of unoccupied binding sites ($n_0(t) \equiv 1 - 7n_{TM}(t) \equiv n_G(t)\bar{g}(t)$, *solid line*) as a function of time, obtained from a stochastic simulation. Parameters: $k_+^N = 1.0 \, \mu M^{-1} \, s^{-1}$, $k_+^P = 50 \, \mu M^{-1} \, s^{-1}$, $k_+^M = 3.0 \, \mu M^{-1} \, s^{-1}$, $k_-^N = 100 \, s^{-1}$, and $\gamma = 1000$. The four graphs show data for different TM concentrations: 0.1, 0.25, 1, and 10 μM. With these values the effective hopping rate is $r_{hop} = 0.28 \, s^{-1}$. The thin lines show the predictions of Eq. 13 for the initial phase, Eq. 7 for the plateau, Eq. 16 for the algebraic regime, and eventually the exact result of Eq. 4 for the equilibrium. The agreement between the theoretical calculations and the simulation becomes very good for concentrations $c \geq 1 \, \mu M$. Simulation data were obtained on a lattice large enough that the results correspond to an infinite system (2^{17} sites and periodic boundary conditions).

binding affinity of an isolated TM molecule has been found to be very low (Weigt et al., 1991), and we may assume

$$K^N c \ll 1. \tag{3}$$

When discussing the dynamics we will neglect all processes where a TM molecule detaches in the middle of a contiguous block, setting $k_-^D \approx 0$.

RESULTS

The equilibrium solution of the problem on an infinite lattice has been known exactly for a long time (McGhee and von Hippel, 1974; Wegner, 1979). The number of attached TM molecules per lattice site n_{TM} (which can assume values between 0 and 1/7) is given by the following implicit equation

$$K^N c = \frac{n_{TM}}{1 - 7n_{TM}} \left(\frac{2(\gamma - 1)(1 - 7n_{TM})}{(2\gamma - 1)(1 - 7n_{TM}) + n_{TM} - R} \right)^6$$

$$\times \left(\frac{2(1 - 7n_{TM})}{1 - 8n_{TM} + R} \right)^2 \tag{4}$$

with

$$R = \sqrt{(1 - 8n_{TM})^2 + 4\gamma n_{TM}(1 - 7n_{TM})}.$$

The average gap size was determined as

$$\bar{g} = \frac{2(\gamma - 1)(1 - 7n_{TM})}{-(1 - 6n_{TM}) + R}. \tag{5}$$

The fraction of unoccupied lattice sites is given as $n_0^{Eq} = 1 - 7n_{TM}$ and the gap density as $n_G^{Eq} = n_0^{Eq}/\bar{g}$. In the limit of very high TM concentrations and nearly full coverage, $n_{TM} \rightarrow 1/7$, the average gap size becomes $\bar{g} \approx 1$.

However, the exact equilibrium configuration is of little value without the knowledge of the time the system needs to equilibrate (relaxation time). Fig. 3 shows the time-dependent filament coverage and gap concentration as obtained from a dynamic Monte-Carlo simulation for different TM concentrations with realistic values for the kinetic constants. As the simulation results show, the dynamics shows an interesting two-stage behavior at high TM concentrations. In the first stage, TM molecules bind to actin wherever there is enough unoccupied space. The
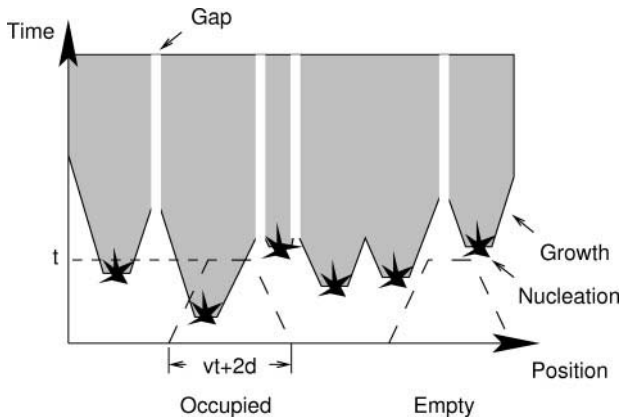
FIGURE 4 Nucleation and growth of TM blocks on actin. Each time the blocks from two different nuclei meet, a gap remains in six of seven cases. A lattice site at time t can be considered as empty if nucleation has not taken place in a trapezium of height t, base $vt + 2d_0$ and top $2d_0$ where v is the sum of growth velocities at both ends and d_0 the size of a nucleus.

first stage is followed by a plateau and the second stage in which reordering of bound TM molecules takes place. In this second stage gaps that inevitably remain after the first stage are healed in an annealing process. The second stage is finally followed by an exponential relaxation into the equilibrium state given by Eq. 4. The second stage is much slower than the first one. We therefore conclude that in many experimental situations the relevant properties of the system are actually determined by the dynamic behavior of the model and not its equilibrium state.

Initial binding

In this section we describe the initial dynamics of TM starting with an empty actin filament. Because a single TM molecule only weakly binds to actin (Eq. 3), nucleation is needed to initiate binding. For its description we use the approach first developed by Kolmogorov (1937) in his "grain growth" model (for review, see Evans, 1993; Privman, 1997). Kolmogorov's model assumes that nucleation is sufficiently slower than grain growth, meaning that grains can grow to large sizes before the growth process is stopped by another grain. It therefore neglects fluctuations in the growth process and assumes a constant growth velocity. The nucleation, on the other hand, is described with its full stochasticity.

Where the blocks growing from two neighboring nuclei meet, there is a probability of $1/7$ that they will match exactly without leaving a gap (Fig. 4). In all other cases, occurring with a total probability of $6/7$ a gap of one to six sites will remain. The number of such gaps should therefore equal $6/7$ of the total number of nuclei. All gap sizes between one and six sites occur with equal probabilities, and the average gap width is 3.5 sites.

We calculate the number of gaps after the initial binding process in the following way. For simplicity we assume that the actin concentration is low enough that the TM concentration in the solution does not change significantly in time (a generalization for a time-dependent solution concentration is discussed in the section Time-Dependent Solution Concentration). Then the nucleation rate r_n and the growth velocity v are constant in time. The probability that a nucleus will be formed on a given site at time t equals the nucleation rate at that time multiplied by the probability that the site has not been occupied previously. The latter equals to the probability that there is no nucleus in a triangle of height t and base vt in the position-time diagram (akin to the light cone frequently used to illustrate independent events in the special theory of relativity) (Fig. 4). To improve the accuracy at relatively high nucleation rates, we can take into account that the nucleus already has a width of $d_0 = 14$ sites, and the triangle then becomes a trapezium with side lengths $2d_0 + vt$ and $2d_0$ and height t.

The probability that no nucleation event takes place within the trapezium is given by the zero term of a Poisson distribution with the expectation value $\bar{N} = r_n(vt/2 + 2d_0)t$, namely $P_0 = \exp(-\bar{N})$. Then the nucleation rate at time t reads

$$\bar{r}_n(t) = r_n P_0(t) = r_n e^{-r_n\left(\frac{vt}{2} + 2d_0\right)t}. \tag{6}$$

The density of gaps per lattice site in the state after initial attachment is then given as

$$n_G^0 = \frac{6}{7}\int_0^\infty dt\, \bar{r}_n(t) = \frac{6}{7}\sqrt{\frac{\pi}{2}}\,\eta\, e^{2d_0^2\eta}\,\mathrm{Erfc}(d_0\sqrt{2\eta})$$

with $\eta = \dfrac{r_n}{v}$ \hfill (7)

and is plotted in Fig. 5. Its asymptotic limits are

$$n_G^0(\eta) = \frac{6}{14d_0} \quad \text{for} \quad \eta \to \infty$$

$$n_G^0(\eta) = \frac{6}{7}\sqrt{\frac{\pi}{2}}\,\eta \quad \text{for} \quad \eta \to 0. \tag{8}$$

Once we have expressed the gap concentration with the nucleation and growth rate, we need to express these with the original model parameters. The total growth velocity v (sum of growth velocities at the $+$ and the $-$ end, expressed in lattice sites per time unit) reads

$$v = 7[(k_+^P + k_+^M)c - (k_-^P + k_-^M)] \approx 7(k_+^P + k_+^M)c. \tag{9}$$

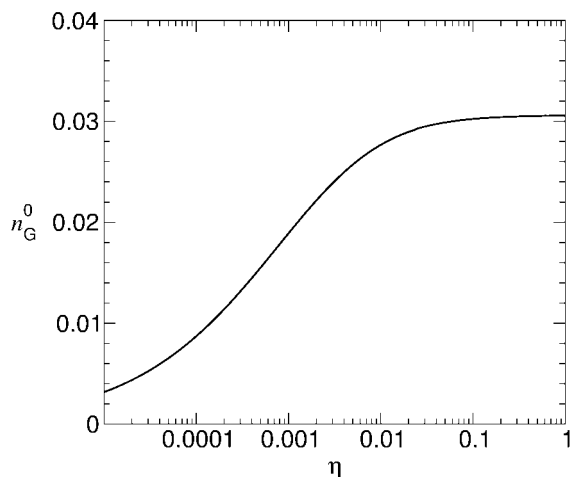In this equation we neglected the effect that uncontiguously bound molecules (which detach after a short time) would

FIGURE 5 The gap density (number of gaps per lattice site) after the initial binding phase, n_G^0 as a function of the parameter $\eta = r_n/v$, as given by Eq. 7.
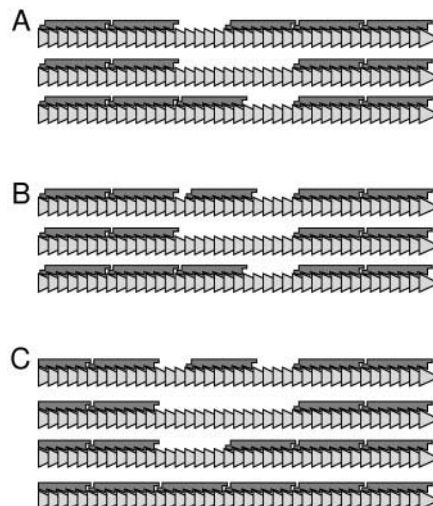

FIGURE 6 Examples of effective reactions that occur after the detachment and attachment of a TM molecule: diffusive step (A); pair coagulation $A + A \to A$ (B); pair annihilation $A + A \to 0$ (C).

have on the growth by blocking the binding sites. This approximation is justified as long as $K^N c \ll 1$.

If $Kc \gg 1$, two molecules bound beside each other already form a stable nucleus, whereas a single one does not (Eq. 3). The nucleation rate r_n can be obtained as the attachment rate of the first molecule multiplied by the probability that a second one binds to its side before the first one detaches and reads

$$r_n = k_+^N \frac{(k_+^P + k_+^M)c^2}{(k_+^P + k_+^M)c + k_-^N}. \tag{10}$$

Together with Eq. 9 we obtain

$$\eta = \frac{k_+^N c}{7((k_+^P + k_+^M)c + k_-^N)}. \tag{11}$$

In the limit of fast equilibration of isolated TM molecules (i.e., if the detachment of an isolated molecule is much faster than the attachment of another one to its side) it simplifies to

$$\eta = K^N c/7 \qquad \text{for} \qquad k_-^P + k_-^M \ll (k_+^P + k_+^M)c \ll k_-^N. \tag{12}$$

The values of the plateau gap concentration obtained from Eq. 7 are shown in Fig. 3 (short-dashed line). They show good agreement with the simulation value as long as the assumption $Kc \gg 1$ is fulfilled. We can go even further in our analysis and give an approximation for the time-dependent vacancy concentration. We can estimate the fraction of empty binding sites at time t as the probability that no nucleus has reached that point plus the number of empty sites that remain in gaps between nuclei (on average three

per nucleus). Therefore, we obtain

$$n_0(t) \equiv 1 - 7n_{TM}(t) = e^{-r_n\left(\frac{vt}{2}+d_0\right)t} + 3\int_0^t dt' r_n e^{-r_n\left(\frac{vt}{2}+2d_0\right)t}$$

$$= e^{-r_n\left(\frac{vt}{2}+d_0\right)t} + 3\sqrt{\frac{\pi r_n}{2v}} e^{\frac{2d_0^2 r_n}{v}}$$

$$\cdot \left[\text{Erf}\left(\sqrt{\frac{2r_n}{v}}\left(d_0 + \frac{vt}{2}\right)\right) - \text{Erf}\left(\sqrt{\frac{2r_n}{v}} d_0\right)\right]. \tag{13}$$

The comparison between the prediction of Eq. 13 and the simulation result can be seen in Fig. 3. The agreement becomes very good at concentrations $c \geq 1 \ \mu M$.

Annealing of gaps

By now we have calculated the gap concentration after the initial binding phase. What follows is a process on a much longer time-scale in which TM molecules at edges of the gaps can detach and reattach. If they reattach on the other side of a gap, the gap makes a move of seven sites in one direction (Fig. 6 a). The rate of such diffusive steps to each direction is given as the detachment rate of a TM molecule on, e.g., the minus side of a block multiplied by the probability that a molecule reattaches on the plus side of the other block before another one reattaches to the position where the first one has detached:

$$r_{hop} = k_-^M \frac{k_+^P}{k_+^P + k_+^M} = \frac{1}{K} \frac{k_+^P k_+^M}{k_+^P + k_+^M} = \left(\frac{1}{k_-^P} + \frac{1}{k_-^M}\right)^{-1}. \tag{14}$$

TABLE 1 Size of the joint gap after coagulation of gaps with sizes g_1 and g_2

g_1	g_2					
	1	2	3	4	5	6
1	2	3	4	5	6	–
2	3	4	5	6	–	1
3	4	5	6	–	1	2
4	5	6	–	1	2	3
5	6	–	1	2	3	4
6	–	1	2	3	4	5

If the initial gap sizes g_1 and g_2 are randomly distributed with values between one and six, the probability for annihilation is 1/6. The probability that the joint gap will have a certain size between one and six is always 5/36.

If two gaps, each containing one to six sites with equal probabilities, come together, they can either join to a single gap (Fig. 6 *b*) or, if their total size exactly fits one TM molecule, annihilate (Fig. 6 *c*). If the original gap sizes are g_1 and g_2, then the joined gap has the size $(g_1 + g_2)$ mod 7. All possible combinations of g_1 and g_2 are shown in Table 1. This table shows that if the probabilities of both gap sizes g_1 and g_2 are equally distributed between one and six, the same will hold for the size of the resulting gap g_j. In one of six cases, the two gaps will annihilate, whereas they will form a new gap with the same size distribution in five of six cases. Thus we can represent gaps as particles A, hopping randomly along the lattice and joining or annihilating when two of them meet. We can therefore map our model to a diffusion-annihilation model consisting of following reactions

$$A + A \rightarrow A \qquad \text{probability } 5/6$$

$$A + A \rightarrow 0 \qquad \text{probability } 1/6$$
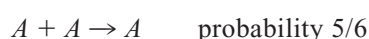
According to Lee (1994) all diffusion-annihilation models of the type $2A \rightarrow lA$ (or generally $kA \rightarrow lA$) belong to the same universality class. In the asymptotic limit the "particle" concentration can be related to that of the exactly solvable $A + A \rightarrow 0$ model (Lushnikov, 1987; Torney and McConnell, 1983) and reads

$$n(t) = \frac{2}{2-l} \frac{1}{\sqrt{8 \pi \bar{r}_{\text{hop}} t}}. \qquad (15)$$

In our case we have to set $l = 5/6$ and $\bar{r}_{\text{hop}} = 7^2 r_{\text{hop}}$. The second relation results from the fact that in each diffusive step a gap jumps over seven sites. We finally obtain

$$n_G(t) = \frac{6}{49 \sqrt{2 \pi r_{\text{hop}} t}} \qquad \text{and} \qquad n_0(t) = 3.5 n_G(t). \qquad (16)$$

Interestingly, the asymptotic particle concentration is independent of its initial value. The gap concentration at long times therefore does not depend on the intermediate gap
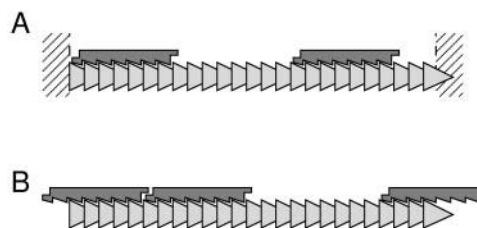
FIGURE 7 Two scenarios for the boundary condition at the ends of an actin filament. (*A*) Hard boundary implies that no TM molecule can bind beyond the end of the actin filament. (*B*) Soft boundary allows TM molecules to bind to the actin end with few segments overhanging.

concentration n_G^0. As our equation reveals, it is even independent of the solution concentration c.

Of course, the mapping to the $A + A \rightarrow lA$ model is only valid as long as the concentration of particles A is well above its equilibrium value. When these come closer, events of pair creation like $A \rightarrow A + A$ become relevant. One can therefore estimate the equilibration time as the time when the vacancy concentration determined by Eq. 16 becomes equal to the equilibrium concentration from Eq. 4. This consideration is only valid if the filaments are long enough that even in equilibrium a considerable number of gaps remains. Otherwise the equilibration time can be estimated as the time in which the gap concentration drops below one per filament.

Fig. 3 also shows the comparison between the result of Eq. 16 and the simulation result. The results agree well for high concentrations where the intermediate plateau and the final equilibrium are far apart. At very high concentrations (not shown, as they would be beyond experimental relevance), there would be an additional power-law regime between the $t^{-1/2}$ law shown here and the final equilibrium. In that regime, processes of the type $A \rightarrow A + A$ become relevant but not yet processes of the type $0 \rightarrow A + A$. The model then becomes equivalent to the noninteracting 7-mer disposition model in which the vacancy density decays according to the mean-field law $\propto t^{-1/6}$ (Nielaba and Privman, 1992). But with experimentally relevant parameters one can see only a slight remnant of this regime.

Finite systems

For now we have assumed infinitely long actin filaments, neglecting all boundary effects. However, in many cases the finite length of actin filaments plays an important role. For example, the length of an actin filament in skeletal muscle is just $\sim$1.1 μm (200 monomers).

There are different possible scenarios how TM molecules should behave at the end of an actin filament (Fig. 7). A hard boundary would mean that a TM molecule cannot bind with any segment overhanging the end of the actin filament. A soft boundary, on the other hand, would

mean that binding of a TM molecule is possible, albeit with a lower affinity, even if less than seven actin sites are free at the end of a filament. The binding constant of a TM molecule partially overhanging the end of the actin filament can be estimated in the following way. If we neglect the entropy gain resulting from the flexibility of the overhanging TM end, the free energy difference between the molecule bound wholly on actin and one with m overhanging segments is

$$\delta G_m - \delta G_0 = \frac{m}{7} J_0 \qquad (17)$$

where J_0 is the binding energy (including hydrophobic contributions) of a TM molecule, which we estimate as $J_0 \approx 20 \ k_B T$. The binding constant for a TM molecule with $7 - m$ bound and m overhanging segments is then

$$K_m = K \exp\left(-\frac{m J_0}{7 k_B T}\right), \qquad (18)$$

giving the values $K_1 \approx 0.057 \ K$, $K_2 \approx 0.0033 \ K$, etc. With the values we use ($K = 10 \ \mu M^{-1}$ and $c \leq 10 \ \mu M$) it turns out that only TM molecules overhanging with one or at most two segments can bind. We therefore conclude that a hard boundary is a good approximation of the real situation even if it might not be exact.

The process of relaxation towards equilibrium on finite filaments differs from that on infinite ones in several aspects. These include the annihilation of gaps when they reach the boundary, the creation of new gaps at the boundary, and the adjustment of the whole TM block to reduce the gaps at the boundary. A discussion of finite-size effects in diffusion-annihilation models can be found in Krebs et al. (1995).

Fig. 8 shows the gap concentration as a function of time for different filament lengths compared with infinitely long filaments. The gap concentration does not differ significantly from infinite filaments before it reaches a value of approximately 1 gap per filament length. After that, the finite-size effects can lower (due to faster gap annihilation at the ends) or raise (due to gap creation at the ends) the gap concentration.

Time-dependent solution concentration

In the previous sections we have assumed that the TM concentration c remains constant during the experiment. This, however, was a simplification as the TM concentration necessarily decreases when some of it gets bound to actin. Situations where TM is added gradually in course of the experiment are conceivable as well.
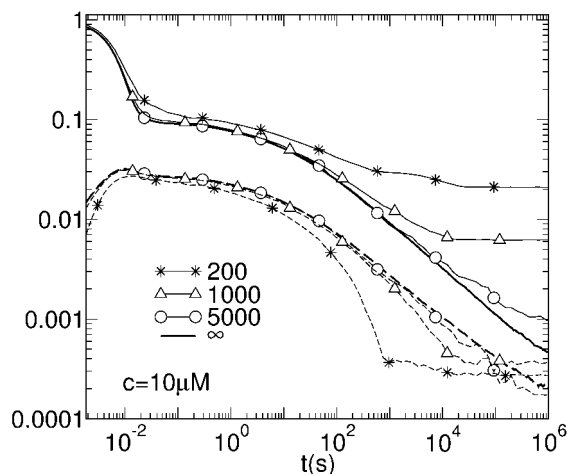
FIGURE 8   Average values of the gap density ($n_G(t)$, *dashed lines*) and fraction of unoccupied binding sites ($n_0(t) \equiv 1 - 7n_{TM}(t)$, *solid lines*) as a function of time for filaments of finite length (200, 1000, and 5000 subunits), compared with results on "infinite" filaments, as obtained from a stochastic simulation. All parameters are the same as in Fig. 3, the TM concentration is $c = 10 \ \mu M$. The empty sites at the end of actin filaments are not counted as gaps, but they do contribute to the fraction of empty sites. The gap density in finite systems does not deviate significantly from infinite systems as long as it is higher than one gap per filament length.

Instead of Eq. 6 we now obtain

$$\bar{r}_n(t) = r_n(c(t))P_0(t) = r_n(c(t)) \exp\left[-\int_0^t r_n(c(t')) \right.$$
$$\left. \times \left(\int_{t'}^t v(c(t''))dt'' + 2d_0\right)dt'\right]. \quad (19)$$

When a part of TM gets bound to actin, the solution concentration decreases according to (the expression for $n_0(t)$ is analog to Eq. 13)

$$c(t) = c_0 - \frac{c_A}{7}(1 - n_0(t))$$

$$= c_0 - \frac{c_A}{7}\left(1 - P_0(t) - 3\int_0^t \bar{r}_n(t')dt'\right) \quad (20)$$

where c_0 denotes the initial TM concentration and c_A the concentration of actin monomers forming the filaments. Eqs. 19 and 20 uniquely determine the TM and gap concentration as a function of time and can be solved numerically. However, in most cases the difference to the solution with a constant concentration is not large. This is due to the fact that the gap concentration is determined by the number of independent nucleation events, and these mostly take place in the initial phase when the solution concentration has not yet dropped significantly. An example is shown in
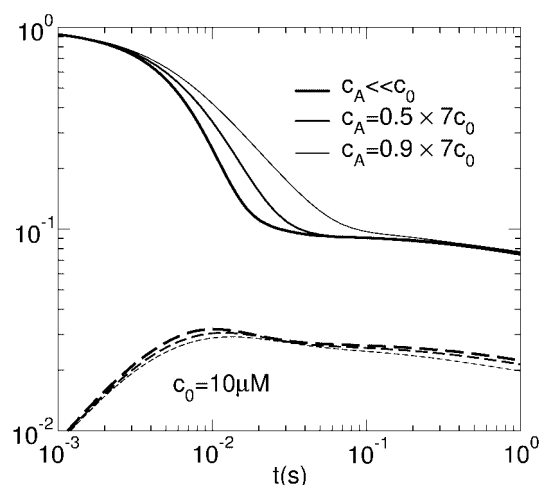
FIGURE 9 Average values of the gap density ($n_G(t)$, *dashed lines*) and fraction of unoccupied binding sites ($n_0(t)$, *solid lines*) as a function of time for different actin concentrations c_A. The simulation takes into account the drop of TM concentration as part of it binds to actin. The results show that the plateau gap concentration is not significantly influenced by this effect.

Fig. 9. There the same curves as in Fig. 3 are shown for the initial TM concentration of $c_0 = 10$ μM and an actin concentration that can take up 50 or 90% of all TM. Although the binding is somewhat slowed down, the plateau gap concentration stays practically the same. In the second (gap annealing) stage the behavior is determined by the detachment rates, which are independent of the concentration. We therefore conclude that the essential features of the system are captured by the model with a constant TM concentration.

DISCUSSION

Table 2 shows the values of model parameters from the literature and the results of our calculation for these values. The equilibrium gap concentration n_G^{Eq} and average gap size $\bar{g}$ only depend on the binding constant K^N, the cooperativity coefficient γ, and the TM solution concentration c. For low concentrations (with a high gap concentration in equilibrium), the system reaches the final state very quickly. These situations are not the subject of our study, and we therefore leave the fields in the table empty. We focus on cases with a high TM coverage of actin filaments. Interestingly, the gap concentration after the initial binding phase n_G^0 only very weakly depends on the TM concentration and other model parameters, its value always being between 0.015 and 0.03 gaps per lattice site (between 2.8 and 5.6 gaps per micron).

The gap concentration during the annealing phase depends almost entirely on the effective hopping rate r_{hop}, given by Eq. 14. The latter is of the order of magnitude of the smaller among the two detachment rates for a molecule at the end of a block, k_-^P and k_-^M. As suggested by Weigt et

al. (1991), there is strong evidence for an asymmetry in the attachment rates on the plus (k_+^P) and the minus end (k_+^M) of a block. We therefore estimate the hopping rate r_{hop} between 0.1 s^{-1} and 0.6 s^{-1}.

In most cases listed in Table 2 the equilibrium gap concentrations were very low. They are only relevant if the filaments are long enough to host at least a few gaps at this low concentration. In most experimental situations this will not be the case. We have shown that in a finite system the gap concentration follows the results for an infinite system as long as the gap concentration is at least a few per filament. We therefore estimate the relaxation time as the time in which the gap density drops below one per filament length. It scales as $t^{Eq} \propto L^2$. For a filament of 1000 lattice sites (5.5 μm) this gives a value between 1 and 6 h. The relaxation time becomes at least 100 times shorter (40–220 s) if one considers a state with 1 gap per 100 lattice sites (roughly two gaps per micron) as equilibrated.

The amount of data gathered in different experimental studies allows us to make quite firm predictions for the vacancy density as a function of time. Our modeling shows that in many relevant experimental situations, especially when using long filaments, the vacancy concentration is much higher than it would be in equilibrium. Actin filaments used in skeletal muscle sarcomeres, on the other hand, are short enough that the TM equilibrates within a minute. Therefore, care has to be taken when the calcium regulation of myosin activity is studied on filaments assembled in vitro, as calcium regulation is by itself a strongly cooperative process and therefore vulnerable to gaps in TM filaments. We also show that with realistic parameters the effect of the initial solution concentration on the vacancy density is rather small (not more than a factor of 2). The only way to eliminate gaps is to give the system enough time to equilibrate (estimated as an hour on long filaments, although the gap concentration already reaches quite low values after a few minutes), or to assemble the actin and the tropomyosin filaments simultaneously.

Unfortunately, in none of the existing studies could the gap concentration be measured directly. But there could be indirect ways to test the predictions of our model. One possibility would be suddenly to decrease the TM concentration (by dilution) or binding affinity to actin (by an increase in the salt concentration) and study the detachment kinetics. As it is almost exclusively the TM molecules next to gaps that detach, the initial detachment rate could be a direct measure for the gap concentration.

To conclude, we have shown that the dynamics of TM binding to actin polymers shows many stages. An initial fast binding phase is followed by a slow annealing process before it reaches the final equilibrium. We could give analytical approximations for the time dependent gap density in all regimes, using elementary nucleation-growth models for the first stage and a mapping to a reaction-diffusion model in the second stage.

TABLE 2 Model parameters used in our simulation (Fig. 3) and their experimental values

	Fig. 3	Weigt et al., 1991*		Hill et al., 1992[#]	
		100 mM KCl		60 mM KCl	300 mM KCl
K^N (μM^{-1})	0.01	0.005	0.026	0.017	0.00058
$k_+^P + k_+^M$ ($\mu M^{-1}\,s^{-1}$)	53	87	38		
k_-^N (s^{-1})	100	100	100		
γ	1000	1000	1000	90	138
k_+^M (μM^{-1})	3.0	3.0	3.0		
r_{hop} (s^{-1})	0.28	0.58	0.11		
$t_{0.001}$ (s)	8400	4100	22,000		
$t_{0.01}$ (s)	84	41	220		
$c = 0.1\ \mu M$					
$\quad n_G^{Eq}$			0.00095		
$\quad \bar g$	86	1000	7.8	510	17,000
$\quad \eta$			0.00036		
$\quad n_G^0$			0.014		
$\quad t^{Eq}$ (s)			24,000		
$c = 1\ \mu M$					
$\quad n_G^{Eq}$	0.00036	0.00055	0.00024		
$\quad \bar g$	3.6	4.9	2.7	13	1600
$\quad \eta$	0.00093	0.00038	0.0027		
$\quad n_G^0$	0.019	0.014	0.023		
$\quad t^{Eq}$ (s)	63,000	14,000	390,000		
$c = 10\ \mu M$					
$\quad n_G^{Eq}$	0.00015	0.00019	0.00012	0.0032	
$\quad \bar g$	2.1	2.3	1.8	3.1	58
$\quad \eta$	0.0023	0.00074	0.0077		
$\quad n_G^0$	0.023	0.017	0.027		
$\quad t^{Eq}$ (s)	360,000	110,000	1.6×10^6		

The upper block shows the input parameters, the second block the quantities that do not depend on TM concentration, i.e., the hopping rate r_{hop} and the time $t_{0.01}$ ($t_{0.001}$) when the gap density reaches 0.01 (0.001) per lattice site. The lower three blocks show the concentration-dependent quantities for three different TM concentrations. These include the equilibrium gap density n_G^{Eq}, the average gap size $\bar g$, the plateau gap density n_G^0, and the equilibration time t^{Eq}. Fields for the gap density are left empty where the equilibrium state is only sparsely covered.
*The two columns show two possible interpretations of the experiment, one with a very low K^N and one with a very high K^N.
[#]Fields for the plateau gap density and equilibration time are left empty because no kinetic data are available.

REFERENCES

Evans, J. W. 1993. Random and cooperative sequential adsorption. *Rev. Mod. Phys.* 65:1281–1329.

Fraser, I. D., and S. B. Marston. 1995. In vitro motility analysis of actin-tropomyosin regulation by troponin and calcium: the thin filament is switched as a single cooperative unit. *J. Biol. Chem.* 270:7836–7841.

Geeves, M. A., and S. S. Lehrer. 1994. Dynamics of the muscle thin filament regulatory switch: the size of the cooperative unit. *Biophys. J.* 67:273–282.

Gordon, A. M., M. A. LaMadrid, Y. Chen, Z. Luo, and P. B. Chase. 1997. Calcium regulation of skeletal muscle thin filament motility in vitro. *Biophys. J.* 72:1295–1307.

Hill, T. L. 1985. *Cooperativity Theory in Biochemistry.*: Springer Series in Molecular Biology. Springer-Verlag, New York.

Hill, L. E., J. P. Mehegan, C. A. Butters, and L. S. Tobacman. 1992. Analysis of troponin-tropomyosin binding to actin: troponin does not promote interactions between tropomyosin molecules. *J. Biol. Chem.* 267:16106–16113.

Hitchcock-deGregori, S. E. 1994. Structural requirements of tropomyosin for binding to filamentous actin. *Adv. Exp. Med. Biol.* 358:85–96.

Hitchcock-deGregori, S. E., and T. A. Varnell. 1990. Tropomyosin has discrete actin-binding sites with sevenfold and fourteenfold periodicities. *J. Mol. Biol.* 214:885–896.

Jin, X., G. Tarjus, and J. Talbot. 1994. An adsorption-desorption process on a line: kinetics of the approach to closest packing. *J. Phys. A.* 27:L195–L200.

Kolmogorov, A. N. 1937. Statistical theory of crystallization of metals. *Bull. Acad. Sci. USSR, Math. Ser.* 1:355–359.

Krapivsky, P. L., and E. Ben-Naim. 1994. Collective properties of adsorption-desorption processes. *J. Chem. Phys.* 100:6778–6782.

Krebs, K., M. P. Pfanmüller, B. Wehefritz, and H. Hinrichsen. 1995. Finite-size scaling studies of one-dimensional reaction-diffusion systems. *J. Stat. Phys.* 78:1429–1470.

Lazarides, E. 1976. Two general classes of cytoplasmic actin filaments in tissue culture cells: the role of tropomyosin. *J. Supramol. Struct.* 5:531(383)–563(415).

Lee, B. P. 1994. Renormalization group calculation for the reaction $kA \rightarrow 0$. *J. Phys. A.* 27:2633–2652.

Lehman, W., V. Hatch, V. Korman, M. Rosol, L. Thomas, R. Maytum, M. A. Geeves, J. E. Van Eyk, L. S. Tobacman, and R. Craig. 2000.

Tropomyosin and actin isoforms modulate the localization of tropomyosin strands on actin filaments. *J. Mol. Biol.* 302:593–606.

Lehrer, S. S., and M. A. Geeves. 1998. The muscle thin filament as a classical cooperative/allosteric regulatory system. *J. Mol. Biol.* 277:1081–1089.

Lushnikov, A. A. 1987. Binary reaction $1 + 1 \rightarrow 0$ in one dimension. *Phys. Lett. A.* 120:135–137.

McGhee, J. D., and P. H. von Hippel. 1974. Theoretical aspects of dna-protein interactions: co-operative and non-co-operative binding of large ligands to a one-dimensional homogeneous lattice. *J. Mol. Biol.* 86:469–489.

McLachlan, A. D., and M. Stewart. 1976. The 14-fold periodicity in α-tropomyosin and the interaction with actin. *J. Mol. Biol.* 103:271–298.

Nielaba, P., and V. Privman. 1992. Random sequential adsorption on a linear lattice: effect of diffusional relaxation. *Mod. Phys. Lett. B.* 6:533–539.

Privman, V., editor. 1997. *Nonequilibrium Statistical Mechanics in One Dimension.* Cambridge University Press, Cambridge, UK.

Privman, V., and P. Nielaba. 1992. Diffusional relaxation in dimer deposition. *Europhys. Lett.* 18:673–678.

Torney, D. C., and H. M. McConnell. 1983. Diffusion-limited reactions in one dimension. *J. Phys. Chem.* 87:1941–1951.

Vibert, P., R. Craig, and W. Lehman. 1997. Steric-model for activation of muscle thin filaments. *J. Mol. Biol.* 266:8–14.

Vilfan, A., E. Frey, and F. Schwabl. 2001a. Relaxation kinetics of biological dimer adsorption models. *Europhys. Lett.* 56:420–426.

Vilfan, A., E. Frey, F. Schwabl, M. Thormählen, Y.-H. Song, E. Mandelkow. 2001b. Dynamics and cooperativity of microtubule decoration by the motor protein kinesin. *J. Mol. Biol.* 312:1011–1026.

Wegner, A. 1979. Equilibrium of the actin-tropomyosin interaction. *J. Mol. Biol.* 131:839–853.

Wegner, A., and K. Ruhnau. 1988. Rate of binding of tropomyosin to actin filaments. *Biochemistry.* 27:6994–7000.

Weigt, C., A. Wegner, and M. Koch. 1991. Rate and mechanism of the assembly of tropomyosin with actin filaments. *Biochemistry.* 30:10700–10707.